ADVANCES IN ATMOSPHERIC SCIENCES, VOL. 23, NO. 4, 2006, 551–560

Preliminary Results of 4-D Water Vapor Tomography in the Troposphere Using GPS

BI Yanmeng* (毕研盟), MAO Jietai (毛节泰), and LI Chengcai (李成才)

Department of Atmospheric Sciences, School of Physics, Peking University, Beijing 100871

(Received 5 July 2005; revised 2 December 2005)

ABSTRACT

Slant-path water vapor amounts (SWV) from a station to all the GPS (Global Positioning System) satellites in view can be estimated by using a ground-based GPS receiver. In this paper, a tomographic method was utilized to retrieve the local horizontal and vertical structure of water vapor over a local GPS receiver network using SWV amounts as observables in the tomography. The method of obtaining SWV using ground-based GPS is described first, and then the theory of tomography using GPS is presented. A water vapor tomography experiment was made using a small GPS network in the Beijing region. The tomographic results were analyzed in two ways: (1) a pure GPS method, i.e., only using GPS observables as input to the tomography; (2) combining GPS observables with vertical constraints or *a priori* information, which come from average radiosonde measurements over three days. It is shown that the vertical structure of water vapor is well resolved with *a priori* information. Comparisons of profiles between radiosondes and GPS show that the RMS error of the tomography is about 1–2 mm. It is demonstrated that the tomography can monitor the evolution of tropospheric water vapor in space and time. The vertical resolution of the tomography is tested with layer thicknesses of 600 m, 800 m and 1000 m. Comparisons with radiosondes show that the result from a resolution of 800 m is slightly better than results from the other two resolutions in the experiment. Water vapor amounts recreated from the tomography field agree well with precipitable water vapor (PWV) calculated using GPS delays. Hourly tomographic results are also shown using the resolution of 800 m. Water vapor characteristics under the background of heavy rainfall development are analyzed using these tomographic results. The water vapor spatio-temporal structures derived from the GPS network show a great potential in the investigation of weather disasters.

Key words: GPS, slant path, water vapor, tomography

doi: 10.1007/s00376-006-0551-y

1. Introduction

Water vapor is the most important greenhouse gas in the climate system of the Earth. It also plays a major role in weather processes due to the large energy transfers related to water evaporation and vapor condensation. The water vapor vertical distribution in the atmospheric column is very important to the above processes. Water vapor in the atmosphere has the characteristic of fast variation in temporal and spatial scales. In general, the vertical profile of water vapor can be obtained by radiosondes. However, data from radiosondes have some disadvantages in describing well the water vapor distribution. The radiosonde stations are a few kilometers to a hundred kilometers apart from each other, and radiosondes are expendable which restricts the number of launches to twice daily (0000 and 1200 UTC) at most stations. Because of these shortcomings, radiosonde measurements inadequately resolve the variability of water vapor, which limit our knowledge in many atmospheric problems. Water vapor observations using meteorological satellites provide larger coverage, but the accuracy is usually not very good. Recently, the development of ground-based GPS (Global Positioning System) meteorology provides a new method for monitoring water vapor variation (Bevis et al., 1992).

Ground-based GPS meteorology, developed by many atmospheric scientists and geodesists, includes three main targets. One is the measurement of precipitable water vapor (PWV) at the zenith direction. The second is the remote sensing of slant-path water vapor (SWV). The third is the retrieval of water vapor three-dimensional structures in the local region employing a GPS network, i.e., water vapor tomography. At present, the technique of measuring PWV is al-

*E-mail: bym@pku.edu.cn

ready proven with a 1–2 mm level of accuracy (Rocken et al., 1993, and Duan and Bevis, 1996). The accuracy is pretty high in describing the variation of column water vapor, however, PWV, as the integrated water vapor over the observation station, does not provide any vertical spatial distribution information, which restricts the application of GPS in atmospheric research. Recently, research of SWV has made great progress. Braun et al. (2003) demonstrated that the accuracy of the GPS remote sensing of SWV is also up to the millimeter level compared with water vapor radiometry (WVR). The applications of SWV include monitoring water vapor variability when a front passes, deep convection development, and moisture transport via low-level jets. In contrast to PWV, SWV represents the three-dimensional distribution of water vapor, but it is still the integrated amount along the slant ray path. Tomography using GPS to retrieve water vapor vertical structure resolves the deficiency of SWV, and time resolution is 30 minutes or less. This method enables GPS to play a major role in current and future atmospheric probing to precisely monitor the atmospheric water vapor distribution.

The first studies of water vapor tomography were performed by Flores et al. (2000). They used data from the Kilauea network in Hawaii on 1 February 1997 and a local $4\times4\times40$ voxel (or box) grid over a region of 400 km^2 and 15 km in height to produce the corresponding four dimensional (4-D) wet refractivity images. Their results were validated by forecast analysis from ECMWF, and they concluded that tomographic techniques can be used to monitor the troposphere in time and space. But in their study, the difference in site elevations (from sea level to 2000 m) was an essential factor in resolving the water vapor structure. Hirahara (2000) also reported tomographic results in the Shigaraki GPS experiment, and the time series of variation in wet refractivity that was shown in his paper was derived from the tomographic method on the 318th and 319th days in 1995 as a cold front was passing. The time resolution in his study was set to two hours, and the tomography only showed a slow variation of wet refractivity. Seko et al. (2000) reported a 'Moving Cell' method in tomography. They moved all cells at some velocity in order to make the distribution of the voxels crossed by GPS signals more impartial. The distribution of water vapor was assumed to be quasi-stationary during the analysis period. They used all the observations in this period to obtain the water vapor deviation. If the absolute water vapor value was needed, other independent instruments such as radiosondes or radiometers had to be available to provide *a priori* average water vapor density. Noguchi et al. (2004) used the moving cell method to probe the troposphere every 10 minutes assuming that the voxel moved at the velocity of the wind. In order to reduce the cost of tomographic instruments, the work of Braun and Rocken (2003) was dedicated to the study of employing single-frequency GPS in tomography. They installed 24 single-frequency GPS receivers across a 40 square kilometer area in the Southern Great Plains region of the United States. Combined with Raman Lidar, the 4D presentation of water vapor density was produced with a 500-m vertical grid and a 30-minute interval. They also indicated that it would be difficult to assess small scale tomographic results of water vapor. Skone and Hoyle (2004) tested the 4D tomography of wet refractivity using a GPS network in Australia. They compared zenith wet delay (ZWD) recovered from tomographic fields with radiosonde ZWD and concluded that the accuracy of ZWD from tomography was 0.3–1.2 cm under the condition of *a priori* vertical information from radiosondes. Champollion et al. (2005) performed a tomographic experiment using the ESCOMPTE GPS network in France. They used the standard atmospheric model for mid-latitude as the vertical constraining conditions. Although the spike in humidity at 4000 m could not be resolved, the tomographic resolutions agreed very well with radiosondes. Bastin et al. (2005) first used GPS tomography to validate the three-dimensional water vapor concentrations from a numerical simulation and to investigate the small-scale evolution of the vertical and horizontal distribution of water vapor during the Mistral/seabreeze transition.

All these studies have proved the feasibility of atmospheric three-dimensional tomography with observations from a GPS network. *A priori* information is required in the tomographic method in order to accurately retrieve the vertical structure of the atmosphere. For example, Braun and Rocken (2003) used the Raman Lidar, Skone and Hogle (2004) used single radiosondes, and Champollion et al. (2005) used the standard atmosphere. In this paper, we present a new method of adding *a priori* information by applying the average results of all radiosonde profiles over some time period as *a priori* profiles. This method makes the *a priori* information not completely depend on one-time measurements by radiosondes. We compare the result of the pure GPS method with that of adding *a priori* information. Tomography with a vertical resolution of 800 m best resolves the structure of water vapor, which turns out to be an important result about tomographic vertical resolution, for similar results in previous works have not been found. Hourly results of tomographic water vapor structure are given in this paper.

Slant SWV is the observable datum for GPS tomography. The method of obtaining SWV is therefore described in section 2. The inverse problem and its solution in the tomography are introduced in section

3. In section 4, we show how the horizontal grids are divided, we present an experiment and analysis of water vapor tomography using a GPS network located in the Beijing region, and then we analyze the water vapor features of a heavy rainfall event. Finally, a discussion and a summary are given in sections 5 and 6, respectively.

2. GPS remote sensing of SWV

GPS satellites broadcast signals for applications in navigation and transferring time. The signals received by ground-based GPS receivers are delayed by the ionosphere and the neutral atmosphere. It is well known that the effect of the ionosphere can be removed by exploiting the known frequency dispersion relations. The delays introduced by the neutral atmosphere can be split into two components: hydrostatic delay and wet delay. These effects on signal propagation through the atmosphere have to be determined because they introduce large errors in positioning estimates. On the other hand, information on the state of the atmosphere is carried by these delays and can be retrieved. Hydrostatic delay can be modeled using surface pressure and temperature with very high accuracy, but the wet component cannot be calculated by using surface meteorological observations.

Slant path delays are modeled as the production of the zenith component and the mapping function, then the gradient terms (Flores et al., 2000). The mapping function is a function of satellite elevation. The gradient term is the reflection of the nonisotropic components of the atmosphere. The slant path wet delay can be modeled as:

$$S_{\rm wd} = m_{\rm w}(e)L_{\rm z,w} + m_{\Delta}(e)(G_{\rm N,w}\cos\phi + G_{\rm E,w}\sin\phi) + R\,, \qquad (1)$$

where e and ϕ are the satellite elevation and azimuth angles, respectively, $m_{\rm w}$ and m_{Δ} are the hydrostatic and wet gradient mapping functions, and the last term R represents the post-fit residues. $G_{\rm N,w}$ and $G_{\rm E,w}$ are the components in the north and east directions of the wet gradient. This equation recreates the slant path delay measurement. The use of residues reflects the deficiency of only using the gradient terms to model the nonisotropic part in the atmosphere. On the other hand, including the residuals will decrease the error of the mapping function in the tomographic solution when the elevation is low.

We process the GPS data using the GAMIT software package, which uses double-difference to remove the clock errors from the satellites and receivers, then outputs the total delays, gradients and residues, etc. The mapping function used is the Niell mapping function (Niell, 1996). SWV is calculated using the method described above.

3. Water vapor tomography using GPS

The main aim of the tomography technique is to provide estimated values of model parameters in individual layers from integrated measurements along different ray paths. This technique has been successfully applied in medical, seismic and ionospheric studies (Flores et al., 2000). Although GPS tomography in the ionosphere has been successfully applied earlier (Ruffini et al., 1998), tomography in the troposphere has many differences in the processing method compared with that in the ionosphere. The retrieval parameter of many previous tropospheric tomographies is wet refractivity (Flores et al., 2000; Hirahara, 2000), but this paper focuses on water vapor density (absolute humidity) in each voxel due to water vapor's importance in the atmospheric sciences. The 4D image of water vapor structure can be directly obtained from the tomographic results.

We defined many regular grids in the vertical and horizontal directions over the ground-based GPS network. The water vapor density in each voxel is unknown, and it is assumed to be constant during a time window (e.g., 1 hour). The observed water vapor amount for each slant path should be equal to the sum of the product of the path length and the water vapor density in each voxel. So a number of observation equations for a time interval will be created together. The water vapor contained in each voxel should be obtained by solving these equations. This is essentially an inverse problem, which is the way to obtain the estimated fields if the integrated water vapor observation is known.

By carefully analyzing this problem, it will be found that these equations cannot be easily solved even though the number of equations is greater than the number of unknown parameters. This is mainly because some voxels may not be crossed by any ray due to the anomalistic positions of satellites in the sky. Therefore, the observational equations are usually undetermined with an ill-condition matrix. In order to get the approximate solution, we assumed that the water vapor density in a voxel is a weighted average of its horizontal neighbors, i.e., it is a smoothing constraint, gince the state of the atmosphere is usually continuous in space.

Including these smoothing conditions, the tomographic linear system is therefore rewritten as:

$$\begin{pmatrix} S_{\rm wv} \\ 0 \end{pmatrix} = \begin{pmatrix} A \\ W \end{pmatrix} X\,. \qquad (2)$$

where $S_{\rm wv}$ is the vector of SWV observations. A is the matrix of the lengths of ray in voxels. W represents the smoothing constraints and X is the unknowns of

water vapor density. We solved the linear system using the least-squares method, and the inverse of the matrix is done using the singular value decomposition (SVD) technique described by Flores et al. (2000).

4. Tomography experiment in the Beijing region

As mentioned above, we utilize four GPS stations in the Beijing region to perform the GPS water vapor tomography experiment. One is the SA34 site, which is located at Peking University and belongs to the SuomiNet program (Ware et al., 2000), and the other sites are QLHD, YSDD and BJFS. The BJFS site is one of the International GPS Service (IGS) tracking stations. Figure 1a presents the detailed locations of the four stations. One meteorological station BJNJ is also shown in the plate, which releases radiosondes twice a day, and its data are compared with ours from the GPS tomographic method in this study. In order to correct or improve the GPS ephemeris and obtain the absolute value of zenith neutral delay at each station, we incorporated five global tracking stations, Kunming (Kunm), Lhasa (Lhas), Urumchi (Urum) and Wuhan (Wuhn), into the data process together with the data from the local regional network. The 5 IGS tracking sites cause the long baselines in the solution to be more than 1500 km.

4.1 *Tomographic grid configurations*

The geometric configuration of the network has a significant impact on water vapor tomography. The division of the horizontal grids should place the stations uniformly in different grids. The size of each grid should not exceed an area of 60×60 km^2. Figure 2 can explain this issue. In general, signals whose elevation angles are greater than 15° will be used in order to remove the multipath effect. If the top height of the tropospheric tomography is up to 8 km, the maximum horizontal size of a grid should be less than 59.7 km. If the grid size exceeds this limit, projections on the ground of all rays are in the same grid. Thus all observation equations are correlated and their solution cannot be determined because the water vapor density in one box is imposed to be uniform and unchanging during the analysis period. In the vertical direction, Flores et al. (2000) indicated that the shortest thickness of a layer should be 350 m. If the length is less than this value, noise will affect the tomographic solutions.

Figures 1a and b show the distribution of the GPS stations used in our experiment and the horizontal grid configuration, respectively. There are six grids in the east-west direction with a grid size of 16 km and five grids in the north-south direction with a grid size of 22 km. To test the ability of the tomography to retrieve the water vapor structure, we use different vertical resolutions with 600-m, 800-m, and 1000-m thicknesses respectively for each layer. There are 12 layers with a top height of 7.2 km using the 600 m resolution, 10 layers with a top height of 8 km using the 800-m resolution, and 8 layers up to 8 km using the 1000-m resolution. Thus, the low tropospheric atmosphere is divided into 420, 300, and 240 voxels or boxes, respectively. In each voxel, the water vapor density is assumed to be constant in a time window. We choose the time interval of one hour considering the conditions of the experiment. A software system named WVATOS (Water Vapor TOmographic Software) has been developed that calculates the slant water vapor, models the data and resolves the inverse problems, etc. After the GPS data are processed using the GAMIT software, the 4D structure of water vapor will be derived by combining them with the surface meteorological data.

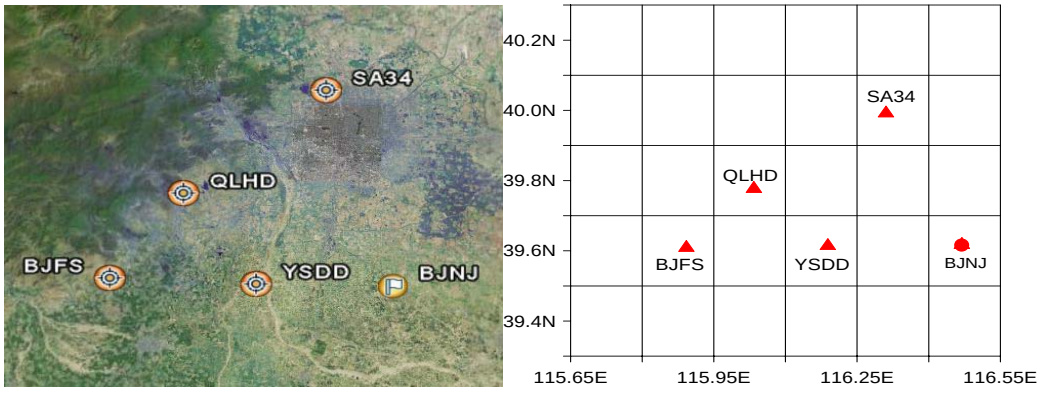

Fig. 1. (a) Map of the locations of the GPS sites in the Beijing region, and (b) representation of the horizontal grids. BJNJ is the radiosonde site.

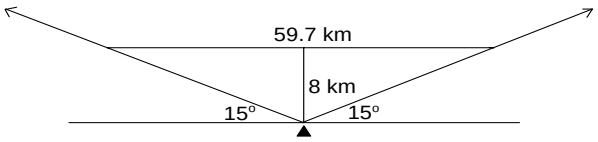

Fig. 2. Schematic representation of signals used in GPS tomography and the horizontal size of one grid.

4.2 *Tomographic solutions and validation*

We processed these GPS data spanning three days, 9–11 July 2004, which were in the summer season in Beijing and where a storm occurred on 10 July. Moisture was abundant and varied greatly against this weather background. The water vapor structure cannot be captured by radiosondes within a few hours but GPS can do this. Using these observations made by GPS, the three-dimensional structure of water vapor was retrieved without any *a priori* information over the GPS network. Figure 3 shows the vertical profile obtained using the resolutions of 600 m and 800 m by GPS tomography at the QLHD site, a nearly central station in our field, during 1200–1300 UTC 10 July 2004. The unit of water vapor density is g m^{-3}. The curve with triangles corresponds to the result using only GPS. Another curve with diamonds represents the radiosonde profile released at 1200 UTC from BJNJ, a national operational meteorological station in Beijing. Compared with the radiosonde results, it is obvious that tomographic solutions using only GPS provide unbelievable results. This illustrates that it is difficult to only use GPS to correctly retrieve water vapor structure. Why is pure GPS not able to get the right water vapor distribution? The reason is mainly dur to the fact that the heights of these sites are similar (maximum difference ∼70 m). The network stations are located on a flat site with low altitudes, which limits the amount of vertical information of water vapor that can be wholly captured by GPS SWV measurements. We impose the assumption that the water vapor in each layer does not have a horizontal variation and only changes in the vertical direction, thus the interchange of two arbitrary layers would lead to the same SWV measurement, and these two distributions cannot be distinguished by the model itself. In order to resolve this problem, we must add *a priori* vertical information that can be obtained from other independent measurements such as profiles from other remote sensing methods or reanalysis meteorological gridded data. The vertical prior constraining information in our study is derived from radiosonde results. We impose the assumption that the water vapor is uniform in each layer and its value is the average measurement of radiosondes during the three days of 9–11 July. After adding *a priori* information, the new tomography equation is presented as,

$$\begin{pmatrix} S_{\rm wv} \\ V_0 \\ 0 \end{pmatrix} = \begin{pmatrix} A \\ B \\ W \end{pmatrix} X \,, \tag{3}$$

where V_0 represents the *a priori* profile and B is the coefficient matrix.

The curve with circles in Fig. 3 is the solutions after adding *a priori* information. It can be seen that the solutions are more reasonable than those only using GPS and agree well with the radiosondes. However, the radiosonde data show a smoother variation than the tomography above 4 km. How can we evaluate this difference above 4 km between the two profiles?

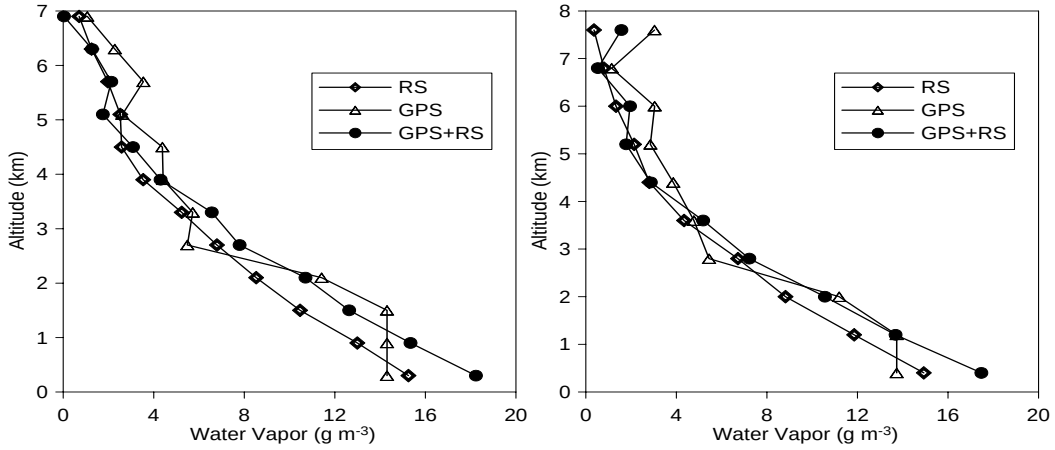

Fig. 3. Tomographic solutions at the QLHD site for 1200–1300 UTC 10 July 2004. (a) 600-m resolution, (b) 800-m resolution. The open-triangle curve represents the solutions only using GPS. The solid-circle curve represents the solutions using GPS and *a priori* information. The solid-diamond curve represents the radiosonde profile launched at 1200 UTC.

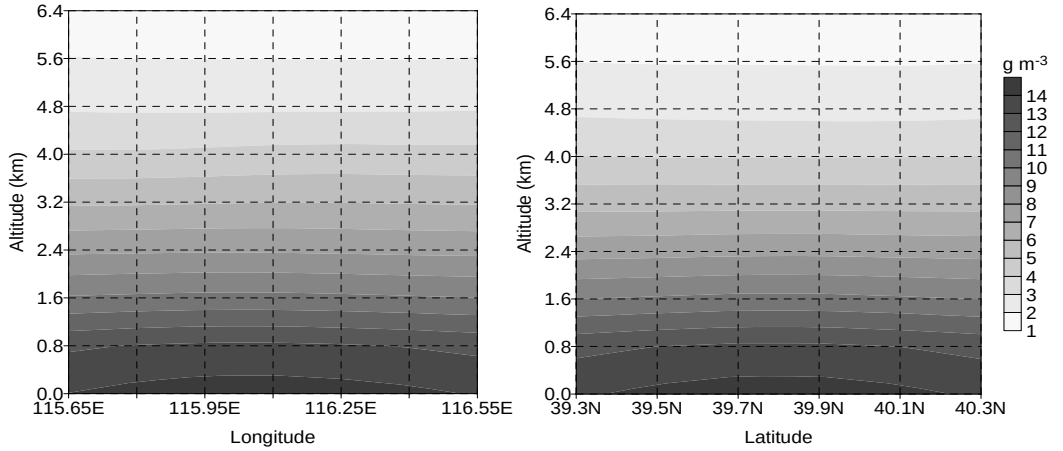

Fig. 4. Vertical cross sections of the tomographic solutions using the 800-m resolution at the QLHD site. (a) in the east-west direction, and (b) in the north-south direction at 1200–1300 UTC 10 July 2004. Water vapor unit is g m^{-3}.

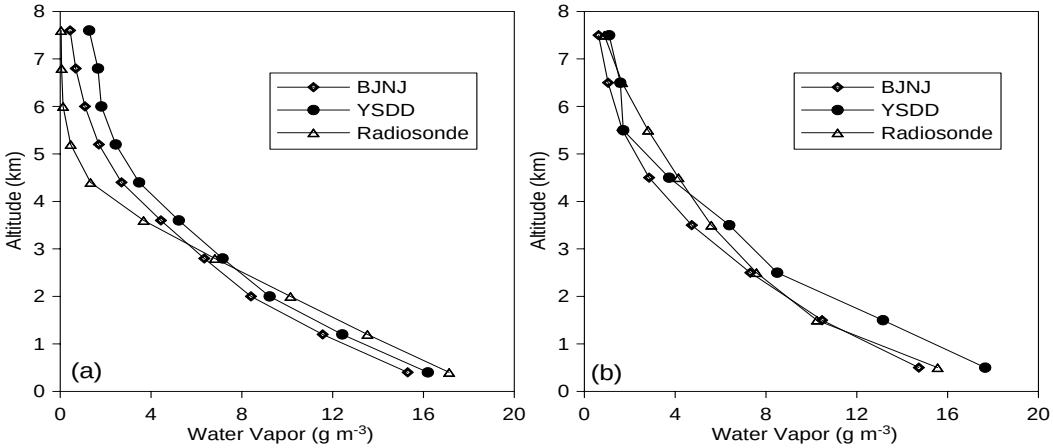

Fig. 5. Water vapor vertical profiles at GPS station YSDD and radiosonde station BJNJ. Resolution in (a) is 800 m at 0000–0100 UTC 10 July 2004. Resolution in (b) is 1000 m at 0000–0100 UTC 11 July 2004.

We believe the tomography may more accurately describe actual atmospheric properties. The humidity sensor installed in a radiosode is usually a capacitor, which is sensitive to humidity but has a lag effect when the balloon is rising. In low humidity situations, the cloud layers will enhance the lag effect and cause the sensed results to be smoother. Therefore, GPS tomography in principle is expected to show unpredictable small-scale behavior of the water vapor content. It can be concluded that the priori vertical constraint information is useful in the determination of the vertical structure of water vapor.

Figure 4 shows two vertical cross sections of water vapor with a resolution of 800 m at the QLHD site along the east-west and north-south directions at 1800–1900 UTC 10 July 2004, respectively. The magnitude of variation in the horizontal layers is as large as 1.5 g m^{-3}. The assessment of these small-scale structures of water vapor in all voxels is difficult because we do not have independent instruments to validate the solutions in all voxels at all times. In order to prove these solutions to some degree, we choose two grids for comparison with the radiosondes. One of the grids is over the radiosonde site BJNJ and the other is over the YSDD site which is separated by one grid (16 km in the longitudinal direction for one grid) from BJNJ (see Fig. 1b). Radiosondes at BJNJ are released twice per day (0000 and 1200 UTC). We therefore select the tomography results at the same time as the radiosondes for comparison. Figure 5 shows the comparison between the tomography and the radiosondes at the BJNJ and YSDD sites. The shown resolutions are 800 and 1000 m. The times in Figs. 5a and 5b are both at 0000 UTC, respectively on 10 and 11 July 2004. It can

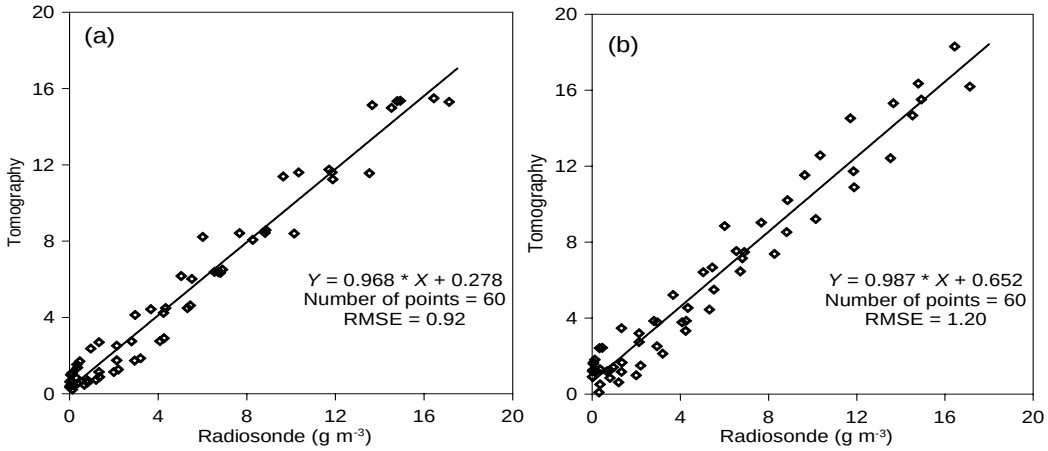

Fig. 6. Scatter-plot between tomography with 800-m vertical resolution and radiosonde measurements. (a) Tomography data is from BJNJ, and (b) tomography data is from YSDD.

be seen that the tomography profiles at the two sites have a good agreement with the radiosonde profiles. It is different from Fig. 3 in that the tomography profiles are smoother. Figure 6 shows the scatter-plot between the two types of profiles at the BJNJ and YSDD sites using 800-m resolution. The RMS errors at the BJNJ and YSDD sites are 0.92 and 1.20 g m^{-3}, respectively. The statistical results including RMS error and average difference (tomography−radiosonde) are shown in Tables 1 and 2. From these comparisons, it can be seen that the magnitude of RMS error is 1–2 mm, and that the agreement between the GPS and radiosondes using three resolutions is almost equivalent, but the 800-m resolution is slightly better than the others. Why is the result of the 800-m resolution better than that of the other two resolutions? As we indicated above, the tomography result is easily affected by noise if the resolution is higher, so the error in the result will be larger. If the resolution is too low (layer thickness is larger), the hypothesis that the water vapor distribution in a given layer is homogeneous during one hour is not appropriate, which also leads to larger error. It should be noted that this kind of comparison is between two different ways to observe the atmospheric water vapor. The tomographic resolution is trying to obtain more detailed spatiotemporal variation of water vapor over a regular grid domain, and its results are easily affected by a few factors such as the local atmospheric states, number of regional sites and geometric configuration of the regional network. If these factors change, the suitable resolution may also change. In addition, the diffences in nature between GPS and radiosonde measurements may cause the observation results to be very different. The GPS profiles extracted from the tomography are mean values of the water vapor over a 1 hour period and over a large volume of air. The radiosonde measurements are instantaneous, but the radiosonde ascent takes about a half an hour to reach a 10 km altitude. Moreover, radiosondes are shifted by the wind (Champollion et al., 2005). In our study, we ignore the effect of wind.

Furthermore, the time series of precipitable water vapor (PWV) in the column from the tomographic fields was calculated by integrating the water vapor in vertical voxels over one site, which is called Tomographic PWV. PWV can also be obtained directly from GPS delays, which is called GPS PWV and stands for an averaged result of all ray paths mapping to the zenith direction. We compared the Tomographic PWV and GPS PWV, and the results of the QLHD site are presented in Fig. 7. The series of Tomographic PWV fits well with the GPS PWV mostly. It should be mentioned that the good matching cannot illustrate the tomographic 3D structure. But if their difference is larger, it can prove that the tomographic 3D structure may not be right.

4.3 *Characteristics of water vapor variability*

It is well known that the convergence and lifting of water vapor are necessary conditions for the production of heavy rainfall. A local disastrous weather event took place in the Beijing region from 0900 to 1200 UTC 10 July 2004. The precipitation intensity

Table 1. Comparison results using different resolutions at radiosonde site BJNJ. Unit is g m^{-3}.

Vertical Resolution	600 m	800 m	1000 m
RMS	1.05	0.92	1.00
Difference	−0.03	0.06	0.07

Table 2. Comparison results using different resolutions at radiosonde site YSDD. Unit is g m^{-3}.

Resolution	600 m	800 m	1000 m
RMS	1.39	1.20	1.27
Difference	0.67	0.59	0.63

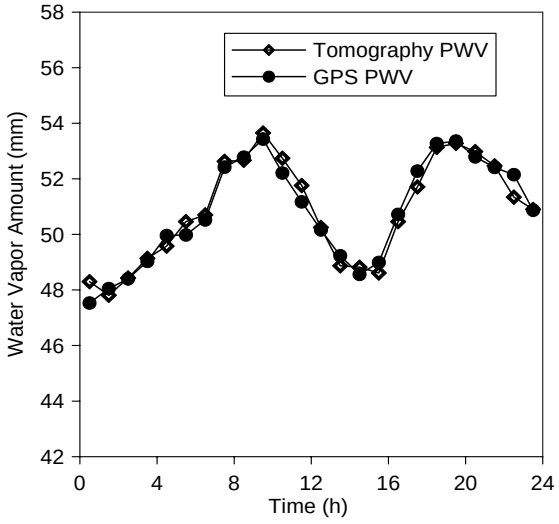

Fig. 7. Comparison of PWV time series derived from tomographic fields and GPS delays at the QLHD site. Time begins at 0000 UTC 10 July 2004. Heavy rainfall occurred at 0900 UTC when the PWV is increasing.

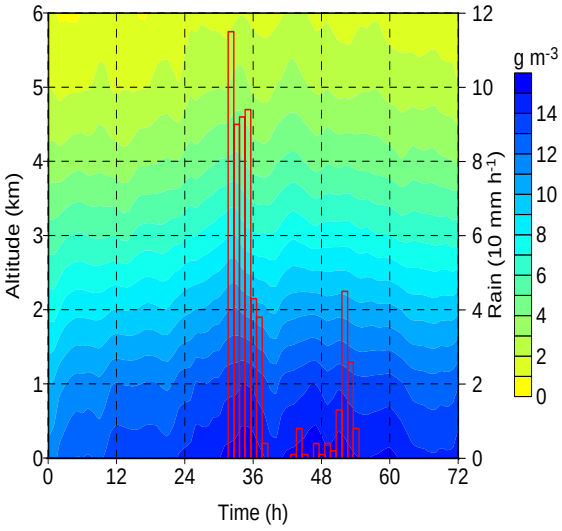

Fig. 8. Tomographic solutions using the 800-m resolution at the QLHD site from 9 to 10 July 2004 (UTC). Hourly rainfall is plotted as a histogram in units of 10 mm h^{-1} and the y-axis of the rainfall is at the right.

measured at many sites exceeded 50 mm h^{-1}. The study of Tao et al. (2004) suggested that this precipitation was caused by a kind of atypical meso-β-scale convective system (MCS), and the height of the cloud top was lower because the brightness temperature at the top of the cloud was higher ($-50°$C) and intensive convection existed within the cloud. It can be seen from Fig. 7 that PWV continuously increases until 0900 UTC when PWV is greater than 53 mm and when the precipitation began. The increase of PWV is about 6 mm within 6–8 hours. Then the PWV shows a decrease that must be attributed to the precipitation. But we cannot determine at which layers the change of water vapor led to the variation of PWV only from the results shown in Fig. 7. Tomographic solutions are helpful in solving this problem. Figure 8 shows the tomographic solutions using the 800-m resolution at the QLHD site from 9 to 11 July 2004, and hourly precipitations are also given. Comparing Fig. 7 with Fig. 8, we can see that the increase of PWV is caused by the change of water vapor at lower layers during the 6-8 hours before the precipitation began; in particular, the water vapor below 3 km shows an obvious increase. And then, the water vapor below 3 km undergoes a brief decrease for about 2 hours after the entire first precipitation event ends at about 38 h in Fig. 8. If we focus on the water vapor content below 1 km, it can be seen from the figure that there are two intervals of maximum water vapor content. The first time interval is at around 35 h and at the same time the maximum rainfall intensity reaches 96 mm h^{-1}. Rainfall also occurs in the other time interval of maximum water vapor content, but the intensity is smaller. This analysis indicates that there was enough water vapor in the lower layer which lifted and resulted in this heavy precipitation. The solutions of the other three sites also show similar results. Therefore, we conclude that the GPS tomographic method can reveal the temporal and spatial variations of water vapor under storm conditions. GPS observation in conjunction with other instruments will open the way to the monitoring and forecasting of meso-scale precipitation.

5. Discussions

Water vapor fields have a significant impact on numerical weather prediction. On the other hand, water vapor fields will delay the GPS signals. Based on this delay information, 4D water vapor fields can be retrieved by the tomographic technique using observations made by a GPS network. Possible applications of water vapor tomography include providing water vapor images for complex weather phenomena or offering good initial conditions for a numerical weather model. Then, forecast accuracy, especially, now-cast accuracy will hopefully improve by combining the water vapor tomographic infomation. At present, ground-based GPS has widely been developed in many fields and the number of receivers is rapidly increasing, which has accelerated the development of GPS meteorology.

GPS tomography is affected by many factors and there are some difficult problems with this technique. One of the problems is the effect of wind. In this paper, we do not consider wind effects and. But the actual atmosphere is always moving in the horizontal

and vertical directions within our spatial and temporal grid. Noguchi et al. (2004) gave a method that considers the effect of horizontal wind. They imposed the assumption that the whole grid moved at the speed of the horizontal wind velocity. But this method cannot resolve the effect of vertical wind because wind velocity is complex and unpredictable. The other problem is that the geometry of the network will affect the tomography. It is difficult to obtain water vapor structure if the GPS network is flat. On the other hand, the spacing of stations has an impact on the ability to perform the tomography. In a perfect network, the spacings among neighbor stations should be equal and cause most of the voxels to be crossed by signal rays. In order to illustrate that, we can assume an extreme case that all the stations are in one grid when the spacings between stations are small enough. This will be equivalent to the use of one site in the tomography. As is well known, it is impossible to only use one GPS station in tomography. Dense GPS stations allow the atmosphere over the network to be divided into many small voxels. In this paper, four GPS stations are used, and grids are large. The thickness of one layer in most tomography studies is 500 m to 1000 m, but in our study, the 800-m resolution in the vertical direction gave the best solution.

6. Conclusions

In this paper, a tomographic experiment was carried out using a local GPS network in the Beijing region. We used the horizontal smoothing conditions in the matrix equations in order to determine the water vapor density of those voxels where the GPS satellite-receiver rays do not cross. Compared with radiosonde measurements, it was found that it is difficult to determine accurately the vertical structure of water vapor only using GPS data in our tomography experiment. We therefore added the *a priori* values in the vertical direction coming from averaged radiosonde measurements released over three days. The profiles obtained by adding the *a priori* information into the tomography equations are compared with the radiosonde data, and they show good agreement. Other independent instruments such as Raman lidar, radio occultation estimation or meteorological satellites can also be used as source of *a priori* information to aid in retrieving the water vapor profiles. Different resolutions in the vertical direction such as 600 m, 800 m and 1000 m were tested. Comparison among them shows that the tomography profile using an 800-m resolution was the best in our experiment. Then, we used this resolution to retrieve four-dimensional structures each hour in the Beijing region for three days. With these tomographic solutions, the characteristics of the water vapor variability in the temporal and spatial scales were analyzed. It was indicated that full water vapor existing in the lower troposphere is the necessary condition for heavy rainfall. Discussion of some tomographic problems was presented.

Water vapor tomography using GPS observations has a potential future in the monitoring and forecasting of meso-scale precipitation. The four-dimensional water vapor fields outputted by tomography are valuable in numerical simulations. They can be used in validating numerical models, inferring water vapor structure, the water cycle, interferometric synthetic aperture radar (InSAR) imaging, and precise positioning. In this paper, it was demonstrated that GPS tomography can help us understand the variability of water vapor when heavy rainfall occurs. GPS tomography should be regarded as a useful tool for meteorologists.

Acknowledgments. The authors would like to acknowledge Massachusetts Institute of Technology (MIT) for their GAMIT package. We thank the SuomiNet program for providing the GPS data at station SA34. We also wish to thank Dr. Fu Yang for providing partial GPS data. We thank Dr. Song Shuli and Dr. Cao Yunchang for their useful discussions and suggestions about the tomographic problem.

REFERENCES

Bastin, S., C. Champollion, O. Bock, P. Drobinski, and F. Masson, 2005: On the use of GPS tomography to investigate water vapor variability during a Mistral/sea breeze event in southeastern France. *Geophys. Res. Lett.*, **32**, L05808, doi:10.1029/2004GL021907.

Bevis, M., S. Businger, T. A. Herring, C. Rocken, R. Anthes, and R. Ware, 1992: GPS meteorology: Remote sensing of atmospheric water vapor using the Global Positioning System. *J. Geophys. Res.*, **97**, 15787–15801.

Braun, J., C. Rocken, and J. Liljegren, 2003: Comparisons of line-of-sight water vapor observations using the Global Positioning System and a pointing microwave radiometer. *J. Atmos. Oceanic Technol.*, **20**, 606–612.

Braun, J., and C. Rocken, 2003: Water vapor tomography within the planetary boundary layer using GPS. International Workshop on GPS Meteorology, 14–17 Jan. 2003, Tsukuba, Japan.

Champollion, C., F. Masson, and M. Bouin, 2005: GPS water vapour tomography: Preliminary results from the ESCOMPTE field experiment. *Atmos. Res.*, **74**, 253–274.

Duan, J., and Bevis, M., 1996: GPS meteorology: Direct estimation of the absolute value of precipitable water. *J. Appl. Meteor.*, **35**, 830–838.

Flores, A., A. Rius, and G. Ruffini, 2000: 4D tropospheric tomography using GPS slant wet delays. *Ann. Geophys.*, **18**, 223–224.

Hirahara, K., 2000: Local GPS tropospheric tomography. *Earth Planets Space*, **52**, 935–939.

Niell, A. E., 1996: Global mapping functions for the atmospheric delay at radio wavelengths. *J. Geophys. Res.*, **101**, 3227–3246.

Noguchi, W., T. Yoshihara, T. Tsuda, and K. Hirahara, 2004: Time-height distribution of water vapor derived by moving cell tomography during Tsukuba GPS campaigns. *J. Meteor. Soc. Japan*, **82**(1B), 561–568.

Rocken, C., R. Ware, T. V. Hove, F. Solheim, C. Alber, and J. Johnson, 1993: Sensing atmospheric water vapor with the Global Positioning System. *Geophys. Res. Lett.*, **20**, 2631–2634.

Ruffini, G., A. Flores, and A. Rius, 1998: GPS tomography of the ionospheric electron content with a correlation functional. *IEEE Trans. Geosci. Remote Sens.*, **36**, 143–153.

Seko, H., S. Shimada, H. Nakamura, and T. Kato, 2000: Three-dimensional distribution of water vapor estimated from tropospheric delay of GPS data in a mesoscale precipitation system of the Baiu front. *Earth and Planets Space*, **52**, 927–933.

Skone, S., and V. Hoyle, 2004: Troposphere modeling in a regional GPS network. presented *at the 2004 International Symposium on GNSS/GPS*, Sydney, Australia 15pp.

Tao Zuyu, Ge Guoqing, Zheng Yongguang, Gao Fan, Wang Yingchun, Chen Mingxuan, Duan Yihong, and Yang Yinming, 2004: Similarities and difference between two disastrous weather events occurred in Beijing and Shanghai July 2004 and the aroused scientific problems (primary research report). *Acta Meteorologica Sinica*, **62**(6), 882–887. (in Chinese)

Ware, R. H., D. W. Fulker, and S. A. Stein, 2000: SuomiNet: A real-time national GPS network for atmospheric research and education. *Bull. Amer. Meteor. Soc.*, **81**(4), 677–694.